# Engineering Stabilized Vascular Endothelial Growth Factor-A Antagonists: Synthesis, Structural Characterization, and Bioactivity of Grafted Analogues of Cyclotides

Sunithi Gunasekera,[†] Fiona M. Foley,[†] Richard J. Clark,[†] Lillian Sando,[†] Louis J. Fabri,[‡] David J. Craik,[†] and Norelle L. Daly*[,†]

*The University of Queensland, Institute for Molecular Bioscience, Brisbane QLD 4072, Australia, and CSL, Richmond, Victoria, Australia*

*Received June 10, 2008*

Cyclotides are plant derived mini-proteins with compact folded structures and exceptional stability. Their stability derives from a head-to-tail cyclized backbone coupled with a cystine knot arrangement of three-conserved disulfide bonds. Taking advantage of this stable framework we developed novel VEGF-A antagonists by grafting a peptide epitope involved in VEGF-A antagonism onto the stable cyclotide framework. Antagonists of this kind have potential therapeutic applications in diseases where angiogenesis is an important component of disease progression, including cancer and rheumatoid arthritis. A grafted analogue showed biological activity in an in vitro VEGF-A antagonism assay at low micromolar concentration and the in vitro stability of the target epitope was markedly increased using this approach. In general, the stabilization of bioactive peptide epitopes is a significant problem in medicinal chemistry and in the current study we have provided insight into one approach to stabilize these peptides in a biological environment.

## Introduction

Peptides are an important source of potential drug leads and biotechnological discovery tools because of their high specificity for particular target receptors and their generally low toxicity. Furthermore, small peptides have the advantage of low immunogenicity compared to larger proteins. However, the use of peptides as pharmaceuticals has been limited in the past due to poor bioavailability and stability under physiological conditions. Several approaches have been attempted to improve the stability of pharmaceutically interesting peptides, including cyclization,[1] retroinverso compounds,[2] and the engineering of biologically active sequences into stable natural scaffolds.[3] The latter approach has been termed "protein grafting" and involves the transfer of a "bioactive" epitope onto the surface of a stable folded protein. The target epitopes may come from a variety of sources, including natural or synthetic peptides or bioactive fragments that are part of larger proteins. In a recent example, an epitope involved in anti-HIV activity was grafted on the surface of a stable homodimeric coiled coil, GCN4 leucine zipper.[4] The resulting α-helical peptide had enhanced stability and displayed antiviral activity similar to the native ligand.

In the current study. we have combined the approaches of cyclization and protein grafting to design novel bioactive peptides with enhanced stability. A limited number of previous studies have used acyclic disulfide-rich peptides as scaffolds for incorporation of non-native sequences,[5−8] but the structure, stability, and toxicity of the grafted analogues has not been extensively studied.[5,6] In this study, we have used the cyclic cystine knot (CCK[a]) scaffold as a grafting template and characterized the analogues in terms of activity, structure, stability, and toxicity.

The CCK scaffold is the core structural motif of the cyclotides,[9] which are a recently discovered family of plant proteins that are ∼30 residues in size, have a cyclic backbone, and three disulfide bonds in a cystine knot arrangement. Approximately 100 cyclotide sequences have been reported so far, with thousands more thought to be present in various plant species.[10] The natural sequence diversity of cyclotides coupled with their extreme chemical, thermal, and enzymatic stability,[11] suggests that the CCK motif is a valuable template on which linear epitopes can be stabilized. Indeed, the cyclotides have been described as a natural combinatorial template based on the large number of variant sequences that are naturally present on a conserved structural core.[12] Cyclotides characterized to date fall into two main subfamilies.[9] Möbius cyclotides, the less common of the two, contain a *cis*-proline that induces a local 180° twist in the backbone resembling a Möbius strip. Cyclotides that lack the proline and consequently the conceptual twist in the backbone form the bracelet subfamily.[13] A third cyclotide subfamily called trypsin inhibitors has been identified based on the conserved CCK motif, but the sequences of these cyclotides are more homologous to a family of noncyclic trypsin inhibitors from squash plants than they are to other cyclotides.[14,15]

In addition to their use as scaffolds, cyclotides have a range of intrinsic biological activities that may also prove useful in pharmaceutical, agricultural, or biotechnological applications. These include uterotonic,[16] anti-HIV,[17] cytotoxic,[18] antimicrobial,[19] and antifouling[20] activities. The natural function of cyclotides in plants has been suggested to be in host defense as they have potent activity against *Helicoverpa* species, caterpillar pests of a range of important crop plants such as corn and cotton.[21−24]

In the current study, we have taken advantage of the stable CCK structure of cyclotides and their natural sequence hypervariability to investigate the potential of the CCK scaffold to accommodate a bioactive epitope. The concept of grafting onto the CCK scaffold is schematically represented in Figure 1. The CCK motif has six intercysteine loops, and in this study we

* To whom correspondence should be addressed. Phone: 61-7-3346 2021. Fax: 61-7-3346 2101. E-mail: n.daly@imb.uq.edu.au.

[†] The University of Queensland, Institute for Molecular Bioscience.

[‡] CSL.

[a] Abbreviations: BOC, *tert*-butyloxycarbonyl; CCK, cyclic cystine knot; DIPEA, diisopropylethylamide; HBTU, 2-(1*H*-benzotriazole-1-yl)-1,1,3,3,-tetramethyluronium hexafluorophosphate; EETI, *Ecballium elaterium* trypsin inhibitor; HF, hydrogen fluoride; HIV, human immunodeficiency virus; HPLC, high-performance liquid chromatography; NMR, nuclear magnetic resonance; VEGF, vascular endothelial growth factor.

10.1021/jm800704e CCC: $40.75 
Published on Web 12/03/2008

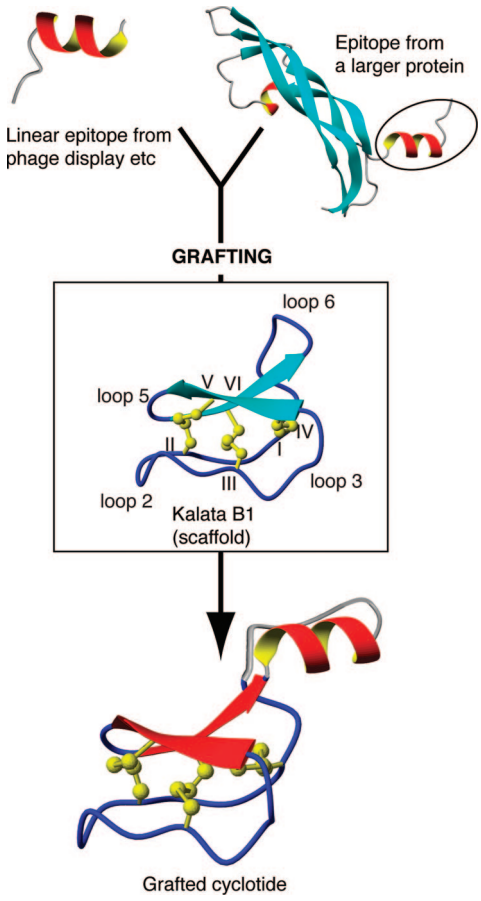


**Figure 1.** Schematic representation of the grafting concept involving insertion of a foreign epitope into the CCK framework. The cystine knot comprises two disulfides ($Cys^{I}$– $Cys^{IV}$ and $Cys^{II}$–$Cys^{V}$) which form a ring that is penetrated by the third disulfide ($Cys^{III}$–$Cys^{VI}$) and in combination with the cyclic backbone forms the cyclic cystine knot (CCK) of the cyclotides. The regions between the cysteine residues are termed "loops" and the four backbone loops labeled in the diagram indicate potential sites of modification in the cyclotide scaffold. The grafting concept is exemplified in the modified cyclotide where a selected loop is replaced with either a linear bioactive epitope or an epitope from a large protein (exemplified by the heparin binding domain of VEGF; PDB code:1kmx).

focused on loops 2, 3, 5, and 6 for the grafting of a biological epitope. We have previously shown that if the backbone is opened in loops 1 or 4, which make up part of the cystine knot motif, the peptide fails to fold into the native conformation.[25]

The biological target epitope chosen for grafting in this study has antiangiogenic activity. Angiogenesis is the complex natural process of forming new blood vessels from preexisting vasculature and involves proliferation, migration, and protease production in endothelial cells. However, unregulated angiogenesis is supportive of a variety of disease states, including solid tumor formation, cancer metastasis, rheumatoid arthritis, and other inflammatory disorders.[26] Thus, designing a stable antagonist to suppress angiogenesis has potential clinical applications.[27,28]

Many positive regulators of angiogenesis, including vascular endothelial growth factor (VEGF), acidic fibroblast growth factor, basic fibroblast growth factor, transforming growth factor-α, transforming growth factor-$\beta$, hepatocyte growth factor, tumor necrosis factor-α, interleukin-8, and the angiopoietins have been identified.[29,30] VEGF-A is a key regulator of physiological as well as pathological angiogenesis, such as that associated with tumor growth. In situ hybridization studies have shown that VEGF mRNA is upregulated in many human tumors.[31,32] The biological function of VEGF-A is mediated through binding to two tyrosine kinase receptors, the kinase domain receptor (KDR, VEGF-R2) and the Fms-like tyrosine kinase (FLT, VEGF-R1).[31] The mitogenic, angiogenic, and permeability-enhancing effects of VEGF-A are mainly mediated through the KDR receptor, whereas FLT is not involved in signaling and appears to function as a decoy receptor to target VEGF cytokine localization. The epitope with antiangiogenesis activity used in this study was the RRKRRR sequence (referred to hereafter as poly-R) that specifically inhibits the interaction of VEGF with the KDR receptor, resulting in antiangiogenesis activity.[33]

Kalata B1, the prototypic cyclotide, was used as the template for grafting the poly-R sequence. The results clearly show that a non-native epitope can be incorporated into the cyclotide scaffold without perturbing the overall fold and results in full biological activity. Furthermore, improvements in stability and removal of unwanted cytotoxic activity were achieved, highlighting the potential of cyclotides as a drug delivery framework.

## Results

The sequences of the grafted analogues of kalata B1 are given in Figure 2. The grafted analogues were named cpr for cyclic poly-R and given a number to distinguish them. Loops 1 and 4 comprise the backbone segments that form the embedded ring of the cystine knot and therefore we chose not to modify these segments. Four grafts were made initially by replacing loops 2, 3, 5, and 6 with the poly-R sequence using solid phase peptide synthesis based on Boc-HBTU chemistry. Two additional grafts in loops 3 and 5 were synthesized based on the results from the initial grafts and analysis of conserved residues in the cyclotide framework. It is important to note that although we use the term grafting, as this reflects the insertion of a foreign epitope into a fixed sequence, in fact each of the grafted peptides was synthesized linearly.

The grafted peptides were assembled with a thioester linker at the C-terminus and with the sequence permuted so as to include an N-terminal cysteine to allow subsequent cyclization. We have previously shown that cyclization can be achieved with a range of C-terminal residues[34,35] and thus there were several options for starting points for the syntheses. Indeed four different start sites were used in the syntheses of the analogues depending on the loop into which the poly-R sequence was incorporated.

**Cyclization, Oxidation, and Characterization of the Grafted Analogues.** The grafted analogues were cyclized and oxidized in a single step reaction in 0.1 M ammonium bicarbonate pH 8.2, 50% isopropanol with either reduced glutathione (0−2 mM) or a mixture of reduced:oxidized glutathione (5:1 ratio). Examples of the RP-HPLC oxidation profiles for the grafted analogues are given in Figure 2. In general, several isomers/peaks were present in the oxidation profiles but the well-resolved latest eluting peaks were initially isolated by RP-HPLC and analyzed because in the folding of acyclic permutants of kalata B1 such late eluting peaks displayed the native fold, in contrast to the earlier eluting peaks.[25]

Of the four initial grafts (cpr1, 2, 4, and 6) cpr1 and cpr6 had late eluting peaks that were subsequently confirmed to have the native structure by chemical shift analysis. A comparison of the secondary shifts of the grafted analogues with native kalata B1 is given in Figure 3 and highlights that the majority of the residues in cpr1 and 6 have similar secondary shifts to kalata B1 (<0.2 ppm). The most significant differences are observed for the loops that have the poly-R sequence grafted

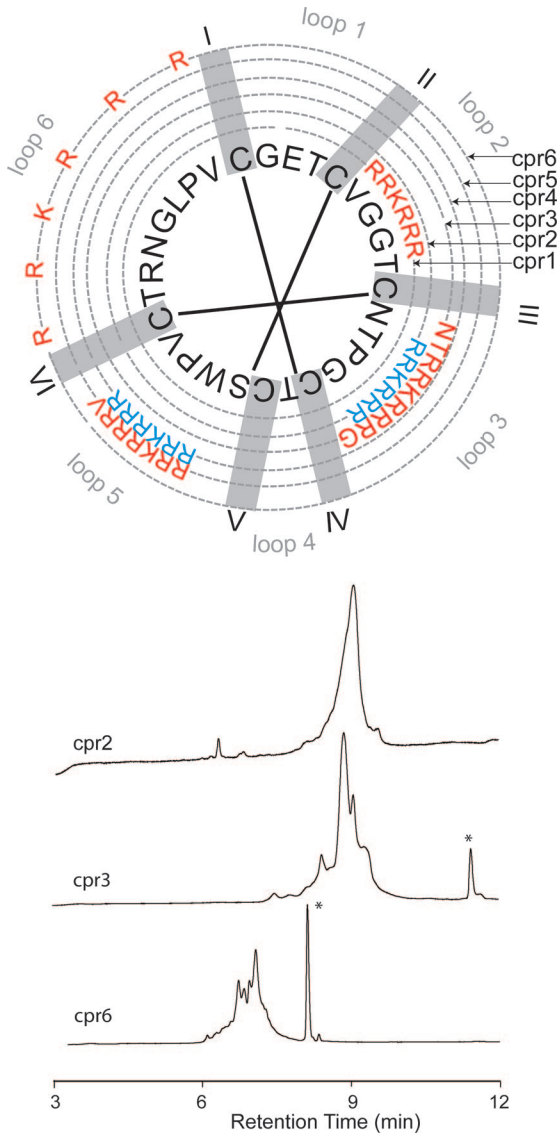


**Figure 2.** Schematic representation of the grafted cyclotide analogues and the analytical-HPLC profiles. The sequence of kalata B1 is shown in the middle with the three disulfides (black lines) interconnecting the cysteines (gray shaded area). The analogues with the poly-R sequence grafted into different loops of the CCK scaffold are shown in concentric circles. The peptides that resulted in folded or partially folded (red) and misfolded (blue) conformations are highlighted. The analytical HPLC profiles of cpr2, cpr3, and cpr6 are shown below the sequences. The highlighted (*) peaks correspond to correctly folded material.

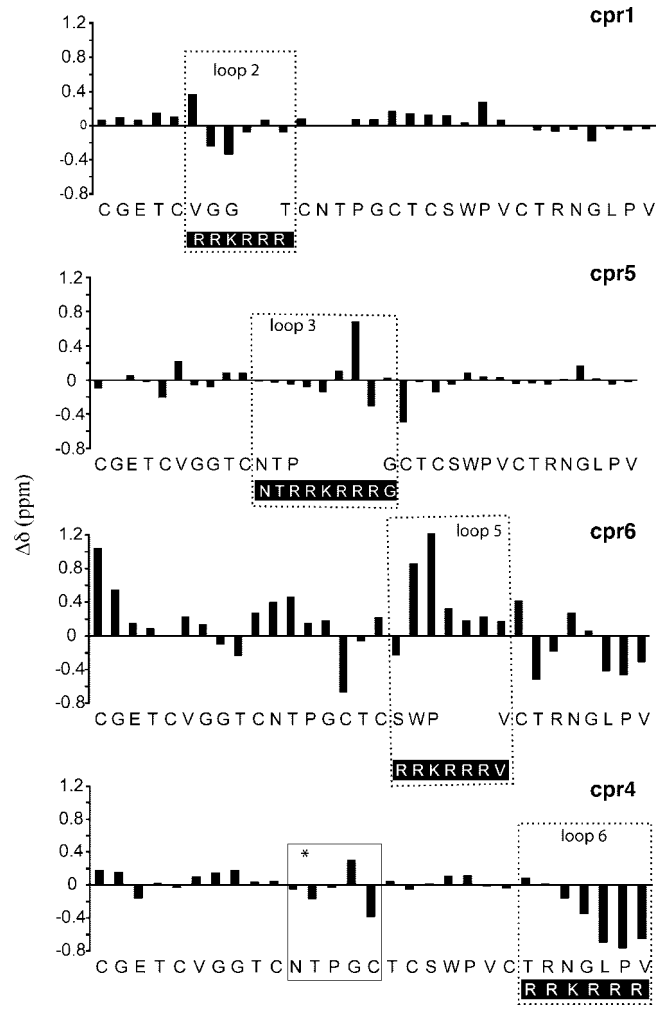


**Figure 3.** Differences between the secondary αH chemical shifts (Δδ) of the grafted analogues and native kalata B1. The secondary αH shifts were calculated by subtracting the random coil shifts[52] from the experimental αH shifts. Each grafted sequence (in white) is shown within black boxes at the site of insertion in the native sequence. Each loop where the insertions with the poly-R epitope was made is boxed in a dashed line and loop 3 of cpr6 is highlighted with an asterisk to indicate the changes in this region as a result of the poly-R insertion into loop 6.

into it, or are in close proximity in the three-dimensional structure as shown for cpr6 with differences in both loops 6 and 3.

cpr2 and cpr4 did not display well-resolved late eluting peaks in their oxidation profiles as shown for cpr2 in Figure 2, and NMR analysis of the major isomers for these analogues indicated the presence of misfolded conformations (i.e., cyclotides are characterized by well-dispersed peaks in the amide region and by contrast the isomers of cpr2 and 4 had significant overlap in this region). To address the issue of misfolding of cpr2 and cpr4, we designed additional analogues with residues flanking the poly-R sequence. The flanking residues were based on conserved residues across the Möbius subfamily. These grafted analogues, cpr3 and cpr5, were cyclized and oxidized, and both displayed late eluting peaks on RP-HPLC. Analysis of these isomers with NMR spectroscopy revealed that the flanking residues have a significant effect on folding as cpr3 has a very similar structure to the native peptide and the fold of cpr5 was partially recovered as shown in Figure 3. The NMR spectra of cpr5 indicate the presence of a relatively well-defined structure based on significant dispersion in the amide region, but there are significant secondary shift differences relative to the native peptide, indicating the overall fold was not completely maintained.

**Antiangiogenesis Assay.** The grafted peptides and kalata B1 were tested in a VEGF competition assay with an engineered cell line (BAF3-VEGF-R2) that proliferates in response to a fixed concentration of VEGF-A (25 nM). The peptides were incubated with cells (50000 cells per well) for 2 days and then the cellular response was measured using an MTS assay. Two control compounds, interleukin-3 and a VEGF-A neutralizing antibody, were also included in the assay. BAF3-VEGF-R2 also proliferates in response to interleukin-3, which is independent of VEGF-A induced cell proliferation. Therefore, interleukin-3 serves as a control to differentiate between VEGF-A antagonism and nonspecific cytotoxity that may be attributed to the grafted analogues. The VEGF neutralizing antibody was used as a positive control to compare the potency of VEGF antagonism

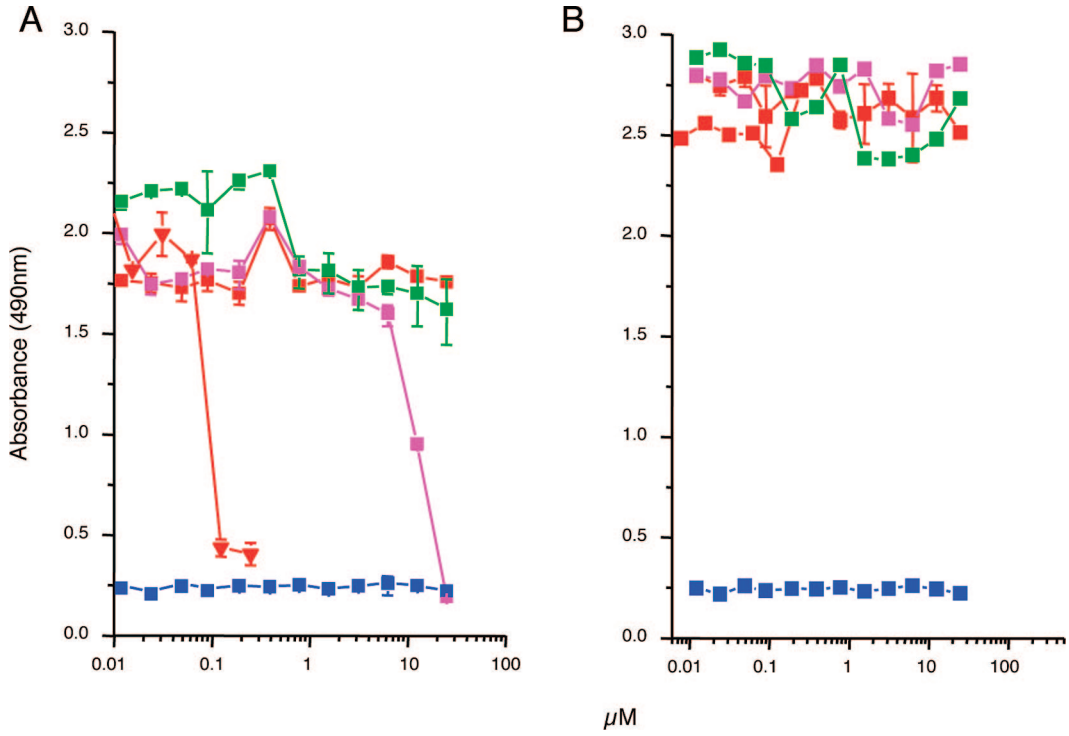


**Figure 4.** Competition of human VEGF-A165 on BAF3/VEGF-R-2 cells by cpr3. BAF3/VEGF-R-2 cells ($4 \times 10^4$/well) incubated with VEGF-A (25 nM) (A) or IL-3 (B) were used for the assay. (A) The inhibition of VEGF-A induced cell proliferation by cpr3 (red square) and VEGF-A neutralizing antibody (avastin) (red triangle) along with the negative control (blue), VEGF-A (red square), and the poly R peptide (green) are shown in the diagram. Two-fold serial dilutions starting at different concentrations were used for cpr3 (starting at 25 $\mu$M) and the antibody control (starting at 250 nM). (B) No inhibition of interleukin-3 (10 ng/mL) induced cell proliferation was observed for cpr3 or the negative control (blue), IL3 (red square), avastin (red triangle), or the poly R peptide (green).

of the grafted analogues. cpr3 showed significant inhibitory activity with an $IC_{50}$ of 12 $\mu$M against VEGF-A as shown in Figure 4. The linear poly-R epitope and other grafted analogues were significantly less active at the concentrations used for cpr3 in this assay. Neither the linear poly-R epitope nor the analogues inhibited proliferation of BAF3-VEGF-R2 in response to interleukin-3. Kalata B1 was found to be cytotoxic at concentrations above 10 $\mu$M, consistent with previous cell-based assays.[36] Interestingly, the cytotoxicity of the parent peptide kalata B1was removed in the grafted analogues.

**Determination of the Three-Dimensional Structures.** The structure of the most active grafted analogue (cpr3) was calculated to determine any influence of the grafted sequences on the three-dimensional structure. The structure of cpr6 was also determined to allow structural comparison of an inactive graft with an active one. As cpr1 and cpr5 were inactive in the antiangiogenesis assay, the structures of these molecules were not determined. The three-dimensional structures were calculated with the program CNS and an overlay of the 20 lowest energy structures along with a ribbon representation is given in Figure 5. In general, the structures are well-defined, with the structure statistics given in Table 1. The major element of secondary structure in the native peptide is a $\beta$-hairpin with the strands connected by loop 5. The $\beta$-hairpin is conserved in both cpr3 and cpr6 of the grafted analogues. Native kalata B1 has several $\beta$-turns, including a type VIa1 $\beta$-turn in loop 5, a type II $\beta$-turn in loop 3 and a type I′ $\beta$-turn in loop 6. Several of these $\beta$-turns are conserved in the grafted analogues. cpr3 and cpr6 both display a type VIa1 $\beta$-turn in loop 5 and a type I′ $\beta$-turn in loop 6. The most significant structural difference is that the grafted region of cpr3 is disordered and protrudes from the core of the molecule. cpr6 is structurally more similar to the native peptide than cpr3 as the grafted loop has been decreased from

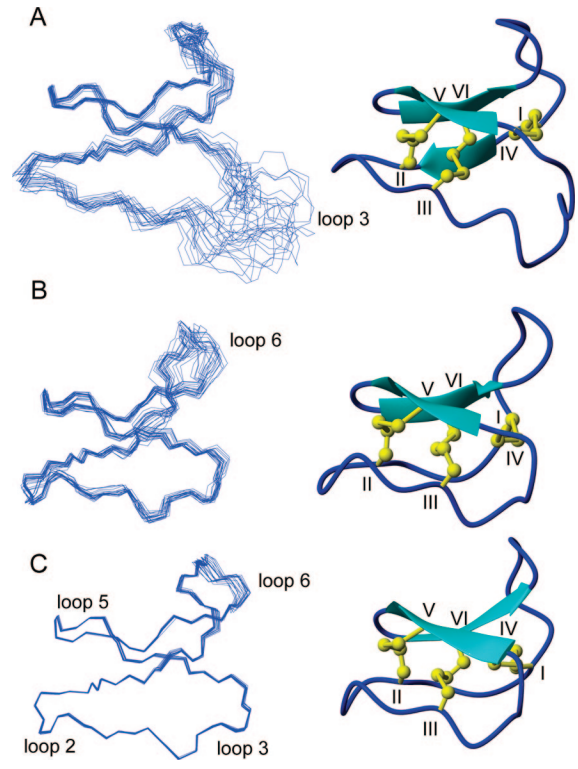


**Figure 5.** Three-dimensional structures of cpr3 and cpr6. A superposition of the 20 lowest energy structures of cpr3 (A), cpr6 (B), and kalata B1 (C) are shown on the left with the corresponding ribbon representations on the right. Structures were determined using NMR spectroscopy and the six cysteine residues are numbered with Roman numerals, the disulfide bonds shown in ball-and-stick format, and the $\beta$-strands shown as arrows.

**Table 1.** NMR Refinement Statistics for cpr3 and cpr6

| NMR distance and dihedral constraints | cpr3 | cpr6 |
|---|---|---|
| distance constraints | | |
| total number of NOEs | 143 | 223 |
| sequential ($i-j=0$) | 86 | 91 |
| medium range ($i-j<4$) | 26 | 39 |
| long range ($i-j\geq 4$) | 31 | 93 |
| total dihedral angle restraints[a] | 25 | 25 |
| structural statistics | | |
| violations (mean and SD) | | |
| distance restraints (Å) | 0.03 ± 0.005 | 0.04 ± 0.004 |
| dihedral angle restraints (deg) | 0.38 ± 0.16 | 0.52 ± 0.22 |
| max dihedral angle violation (deg) | 3 | 3 |
| max distance restraint violation (Å) | 0.3 | 0.3 |
| deviations from idealized geometry | | |
| bond lengths (Å) | 0.004 ± 0.0001 | 0.004 ± 0.003 |
| bond angles (deg) | 0.55 ± 0.02 | 0.67 ± 0.03 |
| impropers (deg) | 0.44 ± 0.03 | 0.51 ± 0.05 |
| average pairwise rmsd[c] (Å) | | |
| backbone | 0.53 ± 0.16 | 0.64 ± 0.2 |
| heavy | 1.15 ± 0.23 | 1.76 ± 0.31 |
| Ramachandran[b] statistics[c] (%) | | |
| favorable region | 62.3 | 77.5 |
| additional allowed region | 37.3 | 20.0 |
| generously allowed region | 0.4 | 2.5 |
| disallowed region | 0 | 0 |

[a] Restraints were implemented with ranges of ± 30°. [b] Procheck_NMR was used to calculate the Ramachandran statistics. [c] cpr3 (residues 1−6, 20−34), cpr6 (residues 1−29).

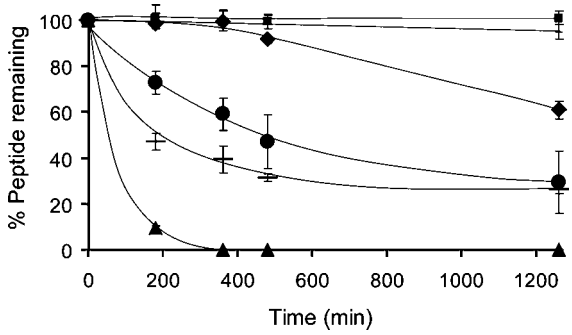


**Figure 6.** Stability of the grafted analogues in human serum. The stability of the grafted peptides in human serum was determined over a >20 h period. Grafted analogues were more stable than the linear epitope (poly-R). The peptides are represented as follows poly-R (triangle), cpr1 (diamond), cpr3 (circle), cpr5 (horizontal line), cpr6 (square), kalata B1 (vertical line).

7 residues in the native peptide to 6 residues, and consequently constraints imposed by the cyclic backbone render this loop similar in structure to the native peptide.

**Serum Stability of the Grafted Analogues.** The stability of the grafted analogues in human serum was investigated for proof-of-concept that cyclotides can be used as a stabilizing framework for bioactive epitopes. The stability of the grafted analogues in serum was compared to the stability of a linear poly-R peptide. The recovery of peptides in human serum varied across the range of peptides tested. The linear epitope degraded in serum to <10% of the initial concentration within the first 3 h of incubation. The percentage peptide remaining in serum was found to be >96% up to 8 h for two of the poly-R grafts tested, indicating their high stability and resistance to enzymatic degradation in serum. The amount of peptide remaining in serum decreased for cpr3 and cpr5 over several hours as shown in Figure 6, but these peptides were still significantly more stable than the linear epitope.

**Hemolytic Assay.** Kalata B1 has been shown to exhibit hemolytic activity,[37,38] and thus we tested the hemolytic activity of the grafted analogues. The results indicate that hemolysis was significantly decreased in all the grafted analogues. Under the conditions of the assay the percentage hemolysis was determined to be ∼50% for kalata B1, ∼7% for cpr1 and cpr6, ∼6% for cpr5, and ∼15% for cpr3 at 50 $\mu$M final peptide concentration. 100% hemolysis was observed at ∼3.5 $\mu$M melittin, which was used as the reference peptide.

## Discussion

The unique CCK topology of the cyclotides has been proposed as a stabilizing framework for biologically active epitopes based primarily on its exceptional stability[39] but prior to this study had not been exemplified. In the current study, we have validated this proposal by successfully grafting a biological epitope having antiangiogenic activity into several backbone loops of the kalata B1 cyclotide framework. The cyclotide framework displayed high versatility for accommodating a foreign sequence without perturbing its global fold. Incorporation of the poly-R epitope within the cyclotide framework markedly increased its stability in human serum. Furthermore, incorporating the epitope within loop 3 of the cyclic cystine scaffold conferred activity in an antiangiogenesis cell-based assay. In addition to conferring a novel bioactivity on the kalata B1 framework, an undesirable bioactivity, namely hemolytic activity, was significantly decreased with the insertion of the foreign epitope. Overall, the study confirms that the CCK framework is a promising scaffold that can stabilize biologically active epitopes while allowing binding to a target receptor.

The most active grafted analogue, cpr3, inhibited VEGF-A stimulated proliferation BAF3-VEGF-R2 assay at low micromolar concentrations. This level of activity is similar to that reported for the linear epitopes with the poly-R sequence antagonizing the VEGF receptor with an $IC_{50}$ of 2−4 $\mu$M.[33,40] Analysis of the structure of cpr3 indicates that the grafted loop (loop 3) is disordered and, based on a lack of NOEs in this region, is presumably a result of flexibility. This apparent flexibility appears likely to be involved in conferring VEGF-A antagonism as the more tightly constrained peptide, cpr6, has lower activity. Alternatively, the scaffold itself in cpr6 may be interfering and preventing activity and by increasing the size of the grafted sequence, such as occurs in cpr3, allows binding to the receptor.

The drawback of the flexibility in the grafted region of cpr3 is that there is a greater probability of enzymatic cleavage due to the lack of a defined structure. Potential cleavage sites within proteins are more susceptible to attack by proteases if they are located in flexible regions of the backbone.[41] Thus, the relative serum instability observed in the loop 3 peptide may be linked to its flexible grafted region. From our findings, it could be inferred that a balance between rigidity and flexibility must be maintained in a grafted loop for it to be biologically active without being subjected to proteolysis by enzymes.

The hemolytic activity of the parent peptide, kalata B1, was significantly reduced in all of the grafted analogues, which involve grafting into four different intercysteine loops. Thus, it appears that each of these loops contain residues that contribute to the hemolytic activity of kalata B1. This finding is consistent with a recent alanine scan study on kalata B1, which reported that residues responsible for hemolytic activity are not confined to a single loop but are located in all six intercysteine loops.[42] These results highlight the potential of the scaffold in drug design as relatively minor sequence changes can remove an undesirable activity.

In terms of the generality of the grafting approach reported here, we note that the poly R epitope chosen for grafting was

originally discovered based on a peptide combinatorial library,[33] has a redundant, repeating nature (poly R), and thus can be considered an "artificial" sequence. On the one hand, it might be argued that this does not provide an insight into the capabilities of the CCK framework for more traditional bioactive eptiopes. On the other hand, we would argue that the tolerance of the framework to accept a highly artificial sequence bodes well for its ability to tolerate natural sequences. Indeed, a recent study clearly demonstrated this tolerance for more natural sequences.[35] In that case, loop 5 was substituted with the sequence SKNK to modulate the hydrophobic properties of the loop. Other studies in our laboratory have involved grafting into loops 2, 5, and 6 (unpublished results), providing evidence that multiple loops are amenable to grafting in the CCK framework.

Other small disulfide rich scaffolds have been explored in recent years for their ability to stabilize otherwise unstable linear epitopes. "Knottin" proteins have been studied in detail for their potential to accommodate novel epitopes on their scaffold. Knottins share a common scaffold comprising a small triple-stranded $\beta$-sheet and a disulfide bonded framework. In one study, the knottin peptide charybdotoxin from scorpion was used to present a human CD4 mimetic site.[8] The engineered CD4 mimetic was shown to intervene in the CD4−gp120 interaction and prevent HIV-1 cell entry. In an earlier study, charybdotoxin was used to accommodate an active metal binding site and was shown to retain its native fold after its carbonic anhydrase site was replaced with the metal binding site.[7] Other knottin proteins, *Ecballium elaterium* trypsin inhibitor II (EETI-II)[5] and cellulose binding domain of cellobiohydrolase I from fungus *Trichoderma reesei*,[43,44] have also been successfully utilized for presenting bioactive epitopes. The cyclotides also contain the knottin fold, but differ in that they are backbone cyclized. Overall, use of disulfide-rich scaffolds to stabilize bioactive epitopes is clearly becoming a promising technique in drug design and the cyclotides, with the added bonus of the stabilizing feature of the cyclic backbone, add another dimension to this approach.

## Conclusion

In conclusion, we have confirmed that a range of grafted cyclotide analogues can be synthesized and form a CCK motif that is stable in human serum. The large number of known cyclotide sequences, which can be thought of as nature's combinatorial library of cyclotides, helped to direct the design process of grafted analogues and highlights the utility of this valuable resource. Furthermore, biological activity was maintained in one of the grafted analogues, validating the potential of this framework in drug design. The fact that the epitope grafted into the scaffold differs significantly from the native sequence because of its repeating nature and thus can be regarded as an "artificial" sequence demonstrates that the CCK framework can potentially accommodate a wide range of epitopes and highlights its value as a grafting template.

## Experimental Section

**Peptide Synthesis.** The linear thioester peptides were assembled using manual solid phase synthesis with Boc/HBTU (or HCTU) chemistry on a 0.5 mmol scale.[45] *S*-Trityl-mercaptopropionic acid was attached to the resin as a linker and the trityl group removed with 1:1:48 TIPS:$H_2O$:TFA. Amino acids (4 equiv) were added to the resin using in situ neutralization (DIPEA 5 equiv). Couplings were monitored by the Kaiser ninhydrin test and double coupled where necessary. Peptides were cleaved from the resin (350−400 mg) using HF with cresol and thiocresol as scavengers (HF:cresol: thiocresol; 50:4:1 v/v). The reaction was allowed to proceed at −5−0 °C for 90 min. The HF was removed and the peptide washed with diethylether and dissolved in 50% solvent A (0.5% aqueous TFA)/solvent B (0.45% TFA in 90% acetonitrile/10% $H_2O$) and lyophilized. The crude reduced peptides were purified using RP-HPLC on a Phenomenex Jupiter C18 300 Å 250 mm × 21.2 mm 15 $\mu$M column (8 mL/min 0−80% solvent B over 80 min, eluent monitored at 230 nm). Mass analysis was performed on an ES-TOF Micromass LCT mass spectrometer.

**Oxidation/Cyclization.** Oxidation trials were carried out using 0.1 mg aliquots of peptide in various oxidation buffers at a concentration of 0.1−0.5 mg/mL to determine the most suitable conditions. The oxidation buffers contained 0.1 M ammonium bicarbonate (pH 8.2) and isopropanol (0−50%) with either reduced glutathione (0−2 mM) or a mixture of reduced: oxidized glutathione (5:1 ratio). The yields based on the recovery of the correctly folded form from pure reduced material were 17% for cpr1, 10% for cpr3, 14% for cpr5, and 25% for cpr6.

**NMR Spectroscopy.** The cyclic/oxidized peptides were dissolved in 95% $H_2O/D_2O$ at concentrations ranging from 0.5−1 mM with a pH of approximately 3. $^1$H NMR spectra were recorded on Bruker 500 and 600 MHz spectrometers at 298 K. TOCSY spectra were recorded using a MLEV-17 spin lock sequence with a mixing time of 80 ms, and NOESY spectra were recorded using 100 and 200 ms mixing times. The water signal was suppressed in TOCSY and NOESY spectra using a modified WATERGATE sequence. Two-dimensional results were generally acquired over 6024 Hz and collected into 4096 data points with 512 t1 increments of 32−64 scans. Spectra were processed on a Silicon Graphics Indigo workstation using XWINNMR (Bruker) software.

**Resonance Assignments and Structure Calculation.** Complete $^1$H chemical shift assignments and NOE intensities were obtained from analysis of the TOCSY and NOESY spectra using the program XEASY. Preliminary structures were calculated using a torsion angle simulated annealing protocol within the program DYANA.[46] Final structures were calculated using simulated annealing and energy minimization protocols within CNS version 1.1.[47] The starting structures were generated using random ($\phi$,$\psi$) dihedral angles and energy-minimized to produce structures with the correct local geometry. A set of 50 structures was generated by a torsion angle simulated annealing protocol.[48] This protocol involved a high-temperature phase comprising 4000 steps of 0.015 ps of torsion angle dynamics, a cooling phase with 4000 steps of 0.015 ps of torsion angle dynamics, during which the temperature was lowered to 0 K, and finally an energy minimization phase comprising 500 steps of Powell minimization. Structures consistent with restraints were subjected to further molecular dynamics and energy minimization in a water shell, as described by Linge and Nilges.[49] The refinement in explicit water involved the following steps. First, heating to 500 K via steps of 100 K, each comprising 50 steps of 0.005 ps of Cartesian dynamics. Second, 2500 steps of 0.005 ps of Cartesian dynamics at 500 K before a cooling phase where the temperature was lowered in steps of 100 K, each comprising 2500 steps of 0.005 ps of Cartesian dynamics. Finally, the structures were minimized with 2000 steps of Powell minimization. Structures were analyzed using PROMOTIF[50] and PROCHECK-NMR.[51] The mean structure was calculated in MOLMOL. All analyses of rmsd, secondary structure, and hydrogen bonds were performed with MOLMOL.

**Antiangiogenesis Assay.** BaF/3-VEGF-R2 cells (kindly provided by Dr. Steven Stacker, Ludwig Institute, Melbourne) were grown in Dulbecco's modified Eagle medium, 5% fetal bovine serum, and Geneticin (G418, 1 mg/mL) and seeded into 96 well plates at 4 × 104 cells per well (50 $\mu$L). Cells were stimulated with human VEGF-A (Chemicon, Australia) at a constant concentration of 300 ng/well in the presence of the grafted peptides at varying dilutions (0.01−25 $\mu$M). BaF/3-VEGF-R2 cells were also stimulated with interleukin-3 (10 ng/well) and incubated with the grafted peptides at the corresponding dilution to serve as a nonspecific inhibitory control in an independent experiment. Cells were incubated at 37 °C, 10% $CO_2$ in a humidified incubator for 96 h prior to development of the assay using a MTS reduction assay, (Cell titer 96 AQueous One Solution Assay, Promega). Absorbance was read

at 490 nm. Assays were run in duplicate and repeated three times. $IC_{50}$ values were calculated using Origin (OriginLab Corporation) and varied less than 10% between assays. Although the poly R sequence exhibited activity in the study by Bae et al.[33] under the current assay conditions, no activity was observed up to 50 $\mu$M.

**Serum Stability Assay.** Serum stability assay was carried out in 100% human male serum (Sigma) using a 20 $\mu$M final peptide concentration. The serum was centrifuged at 14000*g* for 10 min to remove the lipid component and the supernatant was incubated at 37 °C for 15 min prior to the assay. Each peptide was incubated in serum at 37 °C and 40 $\mu$L triplicate aliquots were taken out at time points, 0, 3, 6, 8, and 21 h. Each serum aliquot was quenched with 40 $\mu$L of 6 M urea and incubated for 10 min at 5 °C. Then, each serum aliquot was quenched with 40 $\mu$L of 20% trichloroacetic acid and incubated for another 10 min at 5 °C to precipitate serum proteins. The samples were centrifuged at 14000*g* for 10 min, and 100 $\mu$L of the supernatant was analyzed on RP-HPLC using a linear gradient of solvent B (0.3 mL/min flow rate). The control samples contained equivalent amount of peptides in phosphate-buffered saline subjected to the same treatment procedure. The percentage recovery of peptides was detected by integration at 215 nm.

**Hemolytic Assay.** Human erythrocytes were washed with PBS and centrifuged at 4000 rpm several times until a clear supernatant was obtained. A series of test compounds prepared in 2-fold dilutions (starting from 50 $\mu$M) were used for the assay. Triplicate samples were prepared by mixing 20 $\mu$L of test compound with 100 $\mu$L of 0.25% erythrocyte suspension in phosphate-buffered saline. Melittin was used as the positive control and 100% hemolysis was observed with 1% Triton. The mixtures were incubated at 37 °C for 1 h and centrifuged at 150 relative centrifugal force for 5 min. The absorbance of the supernatant (100 $\mu$L) was measured at 415 nm.

**Acknowledgment.** This work was supported by an Australian Research Council (ARC) linkage grant. DJC is an ARC Professorial Fellow. SG is grateful for an International Postgraduate Research Scholarship. NLD was supported by a NHMRC industry fellowship. We thank Rosa Defazio for expert assistance in the BAF3-VEGF-R2 assay and Dr Steven Stacker from the Ludwig Institute for Cancer Research, Melbourne for kindly providing access to BAF3-VEGF-R2 cell line.

**Supporting Information Available:** Grafted peptide purity quantified by RP-HPLC; RP-HPLC traces of cpr1, cpr3, cpr5 and cpr6; mass spectra data for cpr1, cpr3, cpr5, and cpr6. This material is available free of charge via the Internet at http://pubs.acs.org.

## References

(1) Clark, R. J.; Fischer, H.; Dempster, L.; Daly, N. L.; Rosengren, K. J.; Nevin, S. T.; Meunier, F. A.; Adams, D. J.; Craik, D. J. Engineering stable peptide toxins by means of backbone cyclization: Stabilization of the alpha-conotoxin MII. *Proc. Natl. Acad. Sci. U.S.A.* **2005**, *102*, 13767–13772.

(2) Taylor, E. M.; Otero, D. A.; Banks, W. A.; O'Brien, J. S. Retro-inverso prosaptide peptides retain bioactivity, are stable in vivo, and are blood−brain barrier permeable. *J. Pharmacol. Exp. Ther.* **2000**, *295*, 190–194.

(3) Hosse, R. J.; Rothe, A.; Power, B. E. A new generation of protein display scaffolds for molecular recognition. *Protein Sci.* **2006**, *15*, 14–27.

(4) Sia, S. K.; Kim, P. S. Protein grafting of an HIV-1-inhibiting epitope. *Proc. Natl. Acad. Sci. U.S.A.* **2003**, *100*, 9756–9761.

(5) Christmann, A.; Walter, K.; Wentzel, A.; Kratzner, R.; Kolmar, H. The cystine knot of a squash-type protease inhibitor as a structural scaffold for *Escherichia coli* cell surface display of conformationally constrained peptides. *Protein Eng.* **1999**, *12*, 797–806.

(6) Reiss, S.; Sieber, M.; Oberle, V.; Wentzel, A.; Spangenberg, P.; Claus, R.; Kolmar, H.; Losche, W. Inhibition of platelet aggregation by grafting RGD and KGD sequences on the structural scaffold of small disulfide-rich proteins. *Platelets* **2006**, *17*, 153–157.

(7) Vita, C.; Roumestand, C.; Toma, F.; Menez, A. Scorpion Toxins as Natural Scaffolds for Protein Engineering. *Proc. Natl. Acad. Sci. U.S.A.* **1995**, *92*, 6404–6408.

(8) Vita, C.; Vizzavona, J.; Drakopoulou, E.; Zinn-Justin, S.; Gilquin, B.; Menez, A. Novel miniproteins engineered by the transfer of active sites to small natural scaffolds. *Biopolymers* **1998**, *47*, 93–100.

(9) Craik, D. J.; Daly, N. L.; Bond, T.; Waine, C. Plant cyclotides: A unique family of cyclic and knotted proteins that defines the cyclic cystine knot structural motif. *J. Mol. Biol.* **1999**, *294*, 1327–1336.

(10) Simonsen, S. M.; Sando, L.; Ireland, D. C.; Colgrave, M. L.; Bharathi, R.; Goransson, U.; Craik, D. J. A continent of plant defense peptide diversity: Cyclotides in Australian *Hybanthus* (Violaceae). *Plant Cell* **2005**, *17*, 3176–3189.

(11) Colgrave, M. L.; Craik, D. J. Thermal, chemical, and enzymatic stability of the cyclotide kalata B1: The importance of the cyclic cystine knot. *Biochemistry* **2004**, *43*, 5965–5975.

(12) Craik, D. J.; Cemazar, M.; Wang, C. K. L.; Daly, N. L. The cyclotide family of circular miniproteins: Nature's combinatorial peptide template. *Biopolymers* **2006**, *84*, 250–266.

(13) Rosengren, K. J.; Daly, N. L.; Plan, M. R.; Waine, C.; Craik, D. J. Twists, knots, and rings in proteins—Structural definition of the cyclotide framework. *J. Biol. Chem.* **2003**, *278*, 8606–8616.

(14) Felizmenio-Quimio, M. E.; Daly, N. L.; Craik, D. J. Circular proteins in plants—Solution structure of a novel macrocyclic trypsin inhibitor from *Momordica cochinchinensis*. *J. Biol. Chem.* **2001**, *276*, 22875–22882.

(15) Hernandez, J. F.; Gagnon, J.; Chiche, L.; Nguyen, T. M.; Andrieu, J. P.; Heitz, A.; Hong, T. T.; Pham, T. T. C.; Nguyen, D. L. Squash trypsin inhibitors from *Momordica cochinchinensis* exhibit an atypical macrocyclic structure. *Biochemistry* **2000**, *39*, 5722–5730.

(16) Gran, L.; Sandberg, F.; Sletten, K. *Oldenlandia affinis* (R&S) DC—A plant containing uteroactive peptides used in African traditional medicine. *J. Ethnopharmacol.* **2000**, *70*, 197–203.

(17) Gustafson, K. R.; Sowder, R. C.; Henderson, L. E.; Parsons, I. C.; Kashman, Y.; Cardellina, J. H.; Mcmahon, J. B.; Buckheit, R. W.; Pannell, L. K.; Boyd, M. R. Circulin-A and Circulin-B—Novel HIV-Inhibitory Macrocyclic Peptides from the Tropical Tree *Chassalia parvifolia*. *J. Am. Chem. Soc.* **1994**, *116*, 9337–9338.

(18) Lindholm, P.; Goransson, U.; Johansson, S.; Claeson, P.; Gullbo, J.; Larsson, R.; Bohlin, L.; Backlund, A. Cyclotides: A novel type of cytotoxic agents. *Mol. Cancer Ther.* **2002**, *1*, 365–369.

(19) Tam, J. P.; Lu, Y. A.; Yang, J. L.; Chiu, K. W. An unusual structural motif of antimicrobial peptides containing end-to-end macrocycle and cystine-knot disulfides. *Proc. Natl. Acad. Sci. U.S.A.* **1999**, *96*, 8913–8918.

(20) Goransson, U.; Sjogren, M.; Svangard, E.; Claeson, P.; Bohlin, L. Reversible antifouling effect of the cyclotide cycloviolacin O2 against barnacles. *J. Nat. Prod.* **2004**, *67*, 1287–1290.

(21) Jennings, C.; West, J.; Waine, C.; Craik, D.; Anderson, M. Biosynthesis and insecticidal properties of plant cyclotides: The cyclic knotted proteins from *Oldenlandia affinis*. *Proc. Natl. Acad. Sci. U.S.A.* **2001**, *98*, 10614–10619.

(22) Jennings, C. V.; Rosengren, K. J.; Daly, N. L.; Plan, M.; Stevens, J.; Scanlon, M. J.; Waine, C.; Norman, D. G.; Anderson, M. A.; Craik, D. J. Isolation, solution structure, and insecticidal activity of Kalata B2, a circular protein with a twist: Do Mobius strips exist in nature? *Biochemistry* **2005**, *44*, 851–860.

(23) Gruber, C. W.; Cemazar, M.; Anderson, M. A.; Craik, D. J. Insecticidal plant cyclotides and related cystine knot toxins. *Toxicon* **2007**, *49*, 561–575.

(24) Barbeta, B. L.; Marshall, A. T.; Gillon, A. D.; Craik, D. J.; Anderson, M. A. Plant cyclotides disrupt epithelial cells in the midgut of lepidopteran larvae. *Proc. Natl. Acad. Sci. U.S.A.* **2008**, *105*, 1221–1225.

(25) Daly, N. L.; Craik, D. J. Acyclic permutants of naturally occurring cyclic proteins—Characterization of cystine knot and beta-sheet formation in the macrocyclic polypeptide kalata B1. *J. Biol. Chem.* **2000**, *275*, 19068–19075.

(26) Carmeliet, P. Angiogenesis in life, disease and medicine. *Nature* **2005**, *438*, 932–936.

(27) Quesada, A. R.; Munoz-Chapuli, R.; Medina, M. A. Anti-angiogenic drugs: from bench to clinical trials. *Med. Res. Rev.* **2006**, *26*, 483–530.

(28) Ferrara, N.; Kerbel, R. S. Angiogenesis as a therapeutic target. *Nature* **2005**, *438*, 967–974.

(29) Folkman, J.; Shing, Y. Angiogenesis. *J. Biol. Chem.* **1992**, *267*, 10931–10934.

(30) Yancopoulos, G. D.; Davis, S.; Gale, N. W.; Rudge, J. S.; Wiegand, S. J.; Holash, J. Vascular-specific growth factors and blood vessel formation. *Nature* **2000**, *407*, 242–248.

(31) Ferrara, N. Vascular endothelial growth factor: Basic science and clinical progress. *Endocr. Rev.* **2004**, *25*, 581–611.

(32) Dvorak, H. F.; Brown, L. F.; Detmar, M.; Dvorak, A. M. Vascular-Permeability Factor Vascular Endothelial Growth-Factor, Microvascular Hyperpermeability, and Angiogenesis. *Am. J. Pathol.* **1995**, *146*, 1029–1039.

(33) Bae, D. G.; Gho, Y. S.; Yoon, W. H.; Chae, C. B. Arginine-rich anti-vascular endothelial growth factor peptides inhibit tumor growth and metastasis by blocking angiogenesis. *J. Biol. Chem.* **2000**, *275*, 13588–13596.
(34) Daly, N. L.; Clark, R. J.; Plan, M. R.; Craik, D. J. Kalata B8, a novel antiviral circular protein, exhibits conformational flexibility in the cystine knot motif. *Biochem. J.* **2006**, *393*, 619–626.
(35) Clark, R. J.; Daly, N. L.; Craik, D. J. Structural plasticity of the cyclic-cystine-knot framework: implications for biological activity and drug design. *Biochem. J.* **2006**, *394*, 85–93.
(36) Greenwood, K. P.; Daly, N. L.; Brown, D. L.; Stow, J. L.; Craik, D. J. The cyclic cystine knot miniprotein MCoTI-II crosses the plasma membrane by macropinocytosis. *Biopolymers* **2007**, *88*, 537–537.
(37) Daly, N. L.; Love, S.; Alewood, P. F.; Craik, D. J. Chemical synthesis and folding pathways of large cyclic polypeptide: Studies of the cystine knot polypeptide kalata B1. *Biochemistry* **1999**, *38*, 10606–10614.
(38) Barry, D. G.; Daly, N. L.; Clark, R. J.; Sando, L.; Craik, D. J. Linearization of a naturally occurring circular protein maintains structure but eliminates hemolytic activity. *Biochemistry* **2003**, *42*, 6688–6695.
(39) Craik, D. J.; Simonsen, S.; Daly, N. L. The cyclotides: Novel macrocyclic peptides as scaffolds in drug design. *Curr. Opin. Drug Discovery Dev.* **2002**, *5*, 251–260.
(40) Meinecke, R.; Meyer, B. Determination of the binding specificity of an integral membrane protein by saturation transfer difference NMR: RGD peptide ligands binding to integrin alpha(IIb)beta(3). *J. Med. Chem.* **2001**, *44*, 3059–3065.
(41) Hubbard, S. J. The structural aspects of limited proteolysis of native proteins. *Biochim. Biophys. Acta* **1998**, *1382*, 191–206.
(42) Simonsen, S. M.; Sando, L.; Rosengren, K. J.; Wang, C. K.; Colgrave, M. L.; Daly, N. L.; Craik, D. J. Alanine scanning mutagenesis of the prototypic cyclotide reveals a cluster of residues essential for bioactivity. *J. Biol. Chem.* **2008**, *283*, 9805–9813.
(43) Wernerus, H.; Lehtio, J.; Teeri, T.; Nygren, P. A.; Stahl, S. Generation of metal-binding staphylococci through surface display of combinatorially engineered cellulose-binding domains. *Appl. Environ. Microbiol.* **2001**, *67*, 4678–4684.
(44) Lehtio, J.; Teeri, T. T.; Nygren, P. A. Alpha-amylase inhibitors selected from a combinatorial library of a cellulose binding domain scaffold. *Proteins* **2000**, *41*, 316–322.
(45) Schnölzer, M.; Alewood, P.; Jones, A.; Alewood, D.; Kent, S. B. H. In situ neutralization in Boc-chemistry solid phase peptide synthesis. *Int. J. Pept. Protein Res.* **1992**, *40*, 180–193.
(46) Guntert, P.; Mumenthaler, C.; Wuthrich, K. Torsion angle dynamics for NMR structure calculation with the new program DYANA. *J. Mol. Biol.* **1997**, *273*, 283–298.
(47) Brunger, A. T.; Adams, P. D.; Rice, L. M. New applications of simulated annealing in X-ray crystallography and solution NMR. *Structure* **1997**, *5*, 325–336.
(48) Rice, L. M.; Brunger, A. T. Torsion Angle Dynamics—Reduced Variable Conformational Sampling Enhances Crystallographic Structure Refinement. *Proteins* **1994**, *19*, 277–290.
(49) Linge, J. P.; Nilges, M. Influence of nonbonded parameters on the quality of NMR structures: A new force field for NMR structure calculation. *J. Biomol. NMR* **1999**, *13*, 51–59.
(50) Hutchinson, E. G.; Thornton, J. M. PROMOTIF—A program to identify and analyze structural motifs in proteins. *Protein Sci.* **1996**, *5*, 212–220.
(51) Laskowski, R. A.; Rullmann, J. A. C.; MacArthur, M. W.; Kaptein, R.; Thornton, J. M. AQUA and PROCHECK-NMR: Programs for checking the quality of protein structures solved by NMR. *J. Biomol. NMR* **1996**, *8*, 477–486.
(52) Wishart, D. S.; Sykes, B. D.; Richards, F. M. The Chemical-Shift Index—A Fast and Simple Method for the Assignment of Protein Secondary Structure through NMR-Spectroscopy. *Biochemistry* **1992**, *31*, 1647–1651.

JM800704E